sustainability

IMPACT FACTOR 3.9

CITESCORE 5.8

Article

Investigation on the Durability of a Polypropylene Geotextile under Artificial Aging Scenarios

Philipp Scholz, Jana Falkenhagen, Volker Wachtendorf, Robert Brüll and Franz-Georg Simon

Special Issue

Environmental Protection and Sustainable Ecological Engineering

Edited by

Prof. Dr. Slobodan B. Mickovski, Prof. Dr. Olavo F. Santos Jr., Dr. Alejandro Gonzalez-Ollauri and Dr. Jovan Br. Papić

MDPI

https://doi.org/10.3390/su16093559

sustainability

MDPI

Article

Investigation on the Durability of a Polypropylene Geotextile under Artificial Aging Scenarios

Philipp Scholz [1], Jana Falkenhagen [1], Volker Wachtendorf [1], Robert Brüll [2] and Franz-Georg Simon [1,*]

[1] Bundesanstalt für Materialforschung und -prüfung (BAM), 12200 Berlin, Germany; philipp.scholz@bam.de (P.S.); jana.falkenhagen@bam.de (J.F.); volker.wachtendorf@bam.de (V.W.)
[2] Fraunhofer-Institut für Betriebsfestigkeit und Systemzuverlässigkeit LBF, 64289 Darmstadt, Germany; robert.bruell@lbf.fraunhofer.de
* Correspondence: franz-georg.simon@bam.de

Abstract: Geosynthetics are widely used in various civil engineering applications, such as geotextiles in coastal protection, and display a sustainable alternative to natural mineral materials. However, the full benefits of using geosynthetics can only be gained with a long service lifetime of the products. With the use of added stabilizers to the polymers, service lifetimes can be achieved in the range of 100 years. Therefore, accelerated aging methods are needed for the assessment of the long-term performance of geotextiles. In the present study, the behavior of geosynthetic materials made of polypropylene was investigated under artificial aging conditions involving elevated temperatures ranging from 30 to 80 °C, increased oxygen pressures ranging from 10 to 50 bar in water-filled autoclaves, and UV irradiation under atmospheric conditions. ATR-IR spectroscopy was employed to detect the increase in the carbonyl index over various aging durations, indicating the oxidative degradation of the geotextile. The most pronounced increase was observed in the case of aging through UV irradiation, followed by thermal aging. Elevated pressure, on the other hand, had a lower impact on oxidation. High-temperature size exclusion chromatography was utilized to follow the reduction in molar mass under different degradation conditions, and the results were consistent with those obtained from ATR-IR spectroscopy. In polyolefins such as polypropylene, Hindered Amine Stabilizers (HAS) are used to suppress oxidation caused by UV radiation. The quantitative analysis of HAS was carried out using a UV/Vis method and HPLC. The degradation of UV stabilizers during the aging of geotextiles is responsible for the oxidation and the reduction in the molar mass of polypropylene. From the results, it can be concluded that applications of PP geotextile without soil or sand cover might cause the risk of the formation of microplastic particles. Material selection, design, and maintenance of the construction must follow best practices, including the system's removal or replacement at end-of-life. Otherwise, a sustainable use of geotextiles in civil engineering is not possible.

Keywords: geotextiles; microplastic; size exclusion chromatography; accelerated aging

Citation: Scholz, P.; Falkenhagen, J.; Wachtendorf, V.; Brüll, R.; Simon, F.-G. Investigation on the Durability of a Polypropylene Geotextile under Artificial Aging Scenarios. *Sustainability* **2024**, *16*, 3559. https://doi.org/10.3390/su16093559

Academic Editors: Marc A. Rosen, Alejandro Gonzalez-Ollauri, Slobodan B. Mickovski, Olavo F. Santos Jr. and Jovan Br. Papić

Received: 12 February 2024
Revised: 19 April 2024
Accepted: 20 April 2024
Published: 24 April 2024

1. Introduction

Geotextiles are products made of polymeric material that is widely used in geotechnical applications. According to a recent review, more than 1.4 billion m^2 of energy is used every year [1]. More than 90% of the geotextiles worldwide produced are made of polypropylene. The most important functions are in the field of separation, e.g., separation of fine and coarse mineral material, filtration, drainage, and reinforcement. One of the main advantages of using geotextiles in coastal protection is that they are relatively inexpensive and easy to install. A price of 0.75 \$/m^2 was published [2]. They are also durable and can withstand the harsh conditions of coastal environments. These benefits predestine geotextiles attractive for applications with high material demand, such as coastal protection against erosion and scour [3,4]. Geotextiles are typically placed on or near the shore when used in coastal

protection to stabilize sand and prevent erosion. Geotextiles can be used in a variety of coastal protection applications, such as beach nourishment, dune stabilization, and dike construction. Beach nourishment projects often use geotextiles to hold the new sand in place and prevent it from being washed away by waves and currents. Dune stabilization projects use geotextiles to hold the dune in place and protect the beach and nearby properties from storm surges and wave damage. Besides the mentioned economic advantages, geotextiles save mineral materials such as cement, gravel, or lime as alternative construction materials in civil engineering projects. It was estimated that the cumulative energy demand is higher by more than a factor of 2 for a system with gravel in comparison to a system with geotextiles [2]. Transport of the materials plays a significant role in this assessment. Since the 1970s, the application of geotextile sand containers made of woven and non-woven polymer fibers has gained attraction, and various design and experience reports have been published [5–7]. Whereas in some projects, the expectation of durability of the structures was exceeded [7], the failure of certain design structures has been observed after severe weather events [5].

A weak point of the application of geotextiles could be their stability against weathering during service lifetime. In coastal protection projects, the geotextiles are exposed to several factors that may trigger degradation: seawater, tidal waves, sun radiation, and contact with oxygen. Koerner et al. estimated the time where only 50% of the initial mechanical properties are retained (half-life prediction) to a few months only and up to 10 years for products with proper stabilization against photo-oxidation [8]. Poor performance of unstabilized material in the marine environment was shown by Carneiro et al. A full destruction occurred practically within 12 months [9]. Koerner et al. described the end-of-life of geotextiles as a result of degradation in their thickness and failure by cracking and powdering [8]. This could ultimately lead to the unwished generation of microplastic particles [10]. Additionally, a decreased service lifetime also means that the geotextiles need to be replaced more often, negatively impacting their sustainability. However, maintenance measures and quality control are state-of-the-art as shown for several application projects assessed by Hornsey et al. [7]. Widely used stabilizers for polypropylene comprise the group of phenolic antioxidants and hindered amine stabilizers (HAS, often referred to as hindered amine light stabilizers HALS) [11]. The degradation behavior of both types of stabilizers is different [12]. Whereas samples with phenolic stabilization decompose quickly after an induction period with almost unchanged material properties, HAS-stabilized polymers exhibit constant deterioration over time. In the present study, a HAS-stabilized product was examined. The mechanism of action of HAS is described in detail elsewhere [13].

The influence of temperature and UV radiation on the stabilizers in geotextiles was studied by Heindl et al. [14] using lab tests at 50 °C with two different UV light sources in comparison to outdoor testing. It was shown that both have a large impact on the service lifetime. Higher stabilized samples exhibited higher durability.

In an earlier publication, the long-term performance of geotextiles was investigated after accelerated thermo-oxidative aging in an autoclave at elevated temperatures and oxygen pressure. The decline in material properties was assessed by the measurement of the tensile strength [15]. The service lifetime (half-life prediction) was estimated to be more than 300 years there. However, the tests were performed without exposure to light, and photo-oxidation is believed to be the most important degradation process [16]. This is not a problem as long as the applied geotextiles are covered with soil, sand, or something else. The service lifetime could be considerably shorter in uncovered field applications or stored outdoors before mounting. Koerner et al. estimated the ratio of the field half-lives of geomembranes without exposure to sunlight to that with exposure to approximately seven. This ratio could even be higher for geotextiles [8]. Although uncovered applications should be avoided, at least for long-lasting installations, exposed geotextiles are observed in coastal protection measures, see Figure 1.

In our research, we tested the durability of polypropylene geotextiles over time by changing certain factors like UV radiation, temperature, and oxygen levels to better mimic

real-world conditions. This allowed us to estimate the individual contribution of the different factors influencing the durability.

(**a**)

(**b**)

Figure 1. Geotextiles used as cover for gabions in coastal protection. Location: Swetlogorsk, Oblast Kaliningrad, Russian Federation (**a**) total view, (**b**) detail view with uncovered geotextile.

Whereas the oven test at a rather elevated temperature is an established test for testing the long-term behavior of plastics, artificial weathering was applied in comparison, as UV is regarded as a relevant exposure factor. The photooxidative test could bring a lifetime estimation of samples in a shorter test period at more realistic temperatures. The respective impact of oxygen pressure and temperature was studied by autoclave testing.

The focus of the investigation was laid on the chemical alteration of the products by analysis of the change in molar mass by size exclusion chromatography (SEC, also known as gel permeation chromatography, GPC) [17], the decline in stabilizer content, and degree of oxidation by the carbonyl index [18].

2. Materials and Methods

A white polypropylene (PP) geotextile with a mass per unit area of 600 g m^{-2} was used for all experiments. Thickness was 5 mm, water permeability 3 × 10^{-2} m s^{-1}, and maximum tensile strength in machine direction 42 kN m^{-1}. The product was stabilized with HAS. However, concentration and composition were not known. A German manufacturer provided the sample for geosynthetics for application within liner systems on landfill sites and other geotechnical applications, including hydraulic engineering. To visualize the progress of photooxidative aging, PP pellets were also placed in the weathering device but were only inspected visually.

The HAS Chimassorb 944 (CAS 71878-19-8) and 2020 (CAS 192268-46-7) were purchased from Ciba Specialty Chemical Inc. (Basel, Switzerland) and Tiangang Chemicals Europe B.V. (Leuven, Belgium).

2.1. Accelerated Aging

Aging of the geotextile was performed using three different accelerating test methods: (1) Autoclave tests at elevated temperature and oxygen pressure, (2) Long-term storage at elevated temperature in an oven, and (3) Combined thermo-oxidative and photooxidative exposure in a weathering device.

1. Autoclave tests referring back to DIN EN ISO 13438:2005 (method C) [19,20] were performed under a pure oxygen atmosphere with pressures between 10 and 50 bar (samples placed under water), at temperatures between 30 and 80 °C and durations in the range of 14 and 204 days. Deviated from the standard, the tests were performed with distilled water instead of a NaHCO3 solution at a pH of 10, e.g., by Richaud et al. [21]. An overview of the performed aging experiment is given in Table 1. The procedure is described in detail in an earlier publication [15].

Table 1. Duration of accelerated aging in autoclaves in days (numerical values in the table cells) at five different temperatures and pressures.

p (bar)	Temperature (°C)				
	30	**40**	**60**	**70**	**80**
10					14, 61, 89, 204 *
20					27, 54, 82, 140, 197
30			49, 92, 122		27, 37, 47, 77 (197)
40		49, 92, 122			
50	49, 92, 122			49, 92, 122	

* Experiment in triplicate. One experiment was run for 197 days.

2. Samples of the tested geotextile were placed in an oven at 80 °C for 36, 57, 91, 120, 178, and 364 days. The air exchange in the oven OGH 180 (Thermo Fisher Scientific Inc., Waltham, MA, USA) was in the range of 17 m^3 h^{-1}. The test conditions are described in detail elsewhere [22].
3. The combined thermo-oxidative and photooxidative aging was performed using a Global UV-Test 200 weathering device (Weiss Umwelttechnik GmbH, Reiskirchen-Lindenstruth, Germany) at constant (60 ± 1) °C, and (8 ± 5)% relative humidity for 7, 14, 21, 28 and 35 days. The UV exposure was running continuously. The test method is described in detail elsewhere [23]. Principal methods applied in artificial weathering as well as material sensitivities, can be found in [24]. Test conditions represent exposure in a hot and dry climate. While the climate governing the coastal protection application obviously means wet and humid exposure components, their effect on PP was regarded as negligible (though it might have caused an effect on the stabilizer). The hot and dry climate compares to the climate of similar type in the oven test.

The device conforms to the demands given in ISO 4892-3:2016 [25]. The fluorescent lamps used were UVA-340 lamps of ISO 4892, type 1A. The age of the fluorescent lamps at the start of the test was 466 h. Mounting of the sample in the device is depicted in Figure 2.

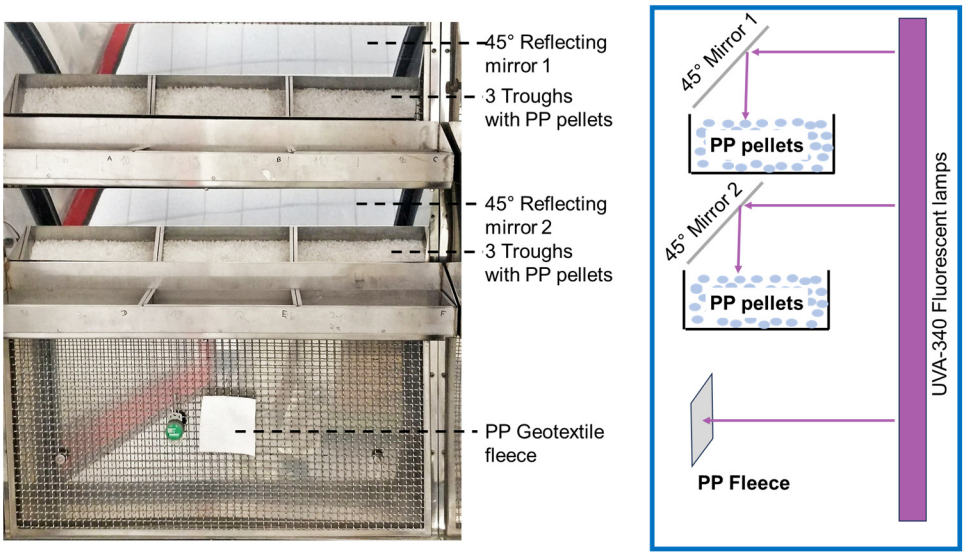

Figure 2. Photo **left**: Front view of mounting of pellets in troughs with 45° mirrors and geotextile fleece sample in the weathering device. Schematics **right**: side view of weathering device and samples.

The pellet material was placed in stainless steel troughs. Six troughs, filled with about 80 g of pellets each, were mounted horizontally on two rows within the weathering device. The UV light, emitted from the vertically oriented fluorescent lamps in the door, was reflected on horizontally mounted 45° reflecting plane aluminum mirrors onto the upper opening of the troughs and hence the pellets. About 30% of UV irradiance is lost by this procedure, which, however, is necessary to irradiate horizontally oriented samples with vertical fluorescent lamps. The three troughs of the upper row received a UV irradiance of 25 W/m^2, and the ones in the lower row of 30 W/m^2. Pellets were taken at intervals of 7 days for further characterization, and the remainder was stirred as several layers (2–3) of pellets were lying on top of each other. Also, the upper and lower rows of troughs and the troughs' positions in the row were rotated. The UV-radiant exposure of the pellet samples after 7, 14, 21, 28, and 35 days on top of the trough was 17, 34, 51, 68, and 85 MJ/m^{2,} respectively, on average. This compares to an annual average maximal exposure in Central Europe of about 180 MJ/m^2 UV. After 21 days of exposure, pellets showed yellowing, pronounced crazing, and cracking on the surface.

Additionally, a piece of about 10 cm × 10 cm geotextile fleece was mounted vertically on the sample chamber's stainless wire mesh back frame into the same weathering device. The small sample size was sufficient to cut off sufficiently sized specimens for the subsequent characterizations. UV-irradiance in the plane of the fleece was 35 W/m^2, resulting in a UV-radiant exposure of 21, 42, 64, 85, and 106 MJ/m^2 for the respective exposure periods of 7, 14, 21, 28, and 35 days. Once a week, a few square centimeters piece was cut and removed for further characterization.

2.2. Determination of Molar Mass Distribution

The molar mass distribution is typically determined using Size Exclusion Chromatography (SEC). For polyolefines, the High-Temperature SEC with different detection methods is a well-established technique. Due to the solubility behavior of these materials, high temperatures and special solvents are essential [26,27].

The molar mass distribution of the polymer was investigated using two similar SEC systems (instrument BAM and instrument LBF). Instrument LBF was a PolymerChar (Valencia, Spain) GPC-IR at 150 °C. The mobile phase used was 1,2,4-trichlorobenzene

(TCB) (Acros Organics, Schwerte, Germany) mixed with ~0.5 g/L butyl hydroxytoluene (BHT, Merck, Darmstadt, Germany) at a flow rate of 1 mL/min. Three PSS POLEFIN analytical, linear XL columns (300 × 8.0 mm, Polymer Standards Service GmbH, Mainz, Germany) were used as stationary phase, and detection was carried out using an IR detector (IR5, PolymerChar). The data sets were evaluated using the WinGPC (PSS) software (UniChrome 8.3) and calibration with polystyrene (EasiCal PS-1, Agilent, Waldbronn, Germany). For the measurements, approximately 6 mg of each polymer sample was independently weighed twice, and 6 mL of the mobile phase was automatically added to it. At the same time, the vials were flushed with N_2. The samples were then dissolved in the autosampler for 1 h with shaking at 160 °C before injection.

Instrument BAM was also a GPC-IR from PolymerChar operated with the same mobile and stationary phase at 160 °C. For calibration, 12 poly(styrene) standards with peak maxima M_p from 266 to 1.2 × 10^7 g/mol (PSS GmbH, now Agilent) were used. The system control standard was (Poly)ethylene NBS 1475.

2.3. ATR-IR Spectroscopy for Determination of Carbonyl Index

ATR-IR spectra were acquired using a Fourier-transform infrared (FTIR) spectrometer (Perkin Elmer System 2000) equipped with an attenuated total reflection (ATR) accessory (DuraSamplIR IITM, Smiths Detection Ltd., Warrington, UK) in the scanning range from 4000 to 650 cm^{-1}. For each sample, 32 scans were recorded using the "Spectrum" software (version 10.4). Given the limited contact area between the ATR diamond crystal and the geotextiles due to their non-woven structure, enhancing signal intensity and reducing the signal-to-noise ratio was crucial. To achieve this, approximately 100 mg of the geotextile samples were placed between two glass slides, which were then heated to approximately 200 °C using a hot air gun for a few seconds. The melted material formed a thin polymer film, which was subsequently measured using ATR-FTIR after cooling to room temperature. Following the measurements, the obtained spectra were normalized and baseline-corrected.

The carbonyl index was calculated from the ratio of the signal intensity of the carbonyl group absorption band at 1715 to 1735 cm^{-1} to the absorption band at 2918 cm^{-1} (C-H stretching band), which was normalized to 1 [18].

2.4. HAS Analysis

A method for the quantification of the Hindered Amine Stabilizers (HAS) Chimassorb 944 based on extraction of HAS and subsequent UV/Vis spectroscopy was suggested by Freitag in 1983 [28] (hereafter called the Freitag method). For the present investigation, 500 mg of the sample (non-woven material) was initially placed in a 250 mL flask with 50 mL of Decalin and a spatula-tip amount of Irganox 1010. The mixture was then stirred at 140 °C under reflux conditions in an oil bath for 40 min. Subsequently, the resulting mixture was transferred to a separatory funnel and shaken with 30 mL of sulfuric acid (0.5 M)/diethanolamine (0.5 vol%) for approximately 1 min. The sulfuric acid phase was retained for the analysis of HAS stabilizers. This process was repeated twice, yielding a total of approximately 90 mL of the sulfuric acid phase. Finally, the solution was filtered and transferred into cuvettes. The quantification of HAS stabilizers was performed through UV/V spectroscopy based on the triazine ring's signal intensity. A UV photometer Specord 200 (Analytik Jena, Jena, Germany) with the software WinAspect (version 2.1) was used for the analysis.

A second analytical method for HAS quantification was based on High-Pressure Liquid Chromatography (HPLC, here: Agilent 1200 series with diode array detector and ChemStation software, version G2170BA). HAS analysis using HPLC is also described elsewhere [29–31]. The initial steps for determining the concentration of HAS using HPLC closely resemble the Freitag method. Specifically, 500 mg of the sample was introduced into a 250 mL flask containing 50 mL of toluene. The mixture was then stirred at 130 °C under reflux conditions in an oil bath for a duration of 40 min. Similar to the Freitag method, the extraction process was performed in triplicate using sulfuric acid/diethanolamine

solutions (concentrations as per the Freitag method). Subsequently, the solution underwent filtration, followed by neutralization with NaOH until a pH of at least 8.0 was achieved. In the subsequent step, the neutralized solution was shaken with 30 mL of chloroform in a separatory funnel for 1 min, and the organic fraction was collected. This process was repeated twice, resulting in a total collection of approximately 90 mL of the organic fraction. Finally, the solvent was removed using a vacuum rotary evaporator. For quantification via HPLC, the HAS stabilizer was dissolved in 1 mL of tetrahydrofuran (THF), serving as the mobile phase. A Zorbax Extend-C18 (4.6 × 150 mm, 5 µm) HPLC column was employed as the stationary phase. Chimassorb 944 was used for calibration, and the concentration was determined based on the signal intensity recorded by the UV detector.

3. Results

3.1. Accelerated Artificial Aging in Autoclaves with Different Temperatures and Oxygen Pressures

The diagram in Figure 3 represents the molar mass distribution of a polypropylene geotextile subjected to accelerated aging within an autoclave at an elevated temperature of 80 °C and a pressure of 10 bar. This method simulates the material's longevity under operational conditions akin to those encountered in coastal protection projects.

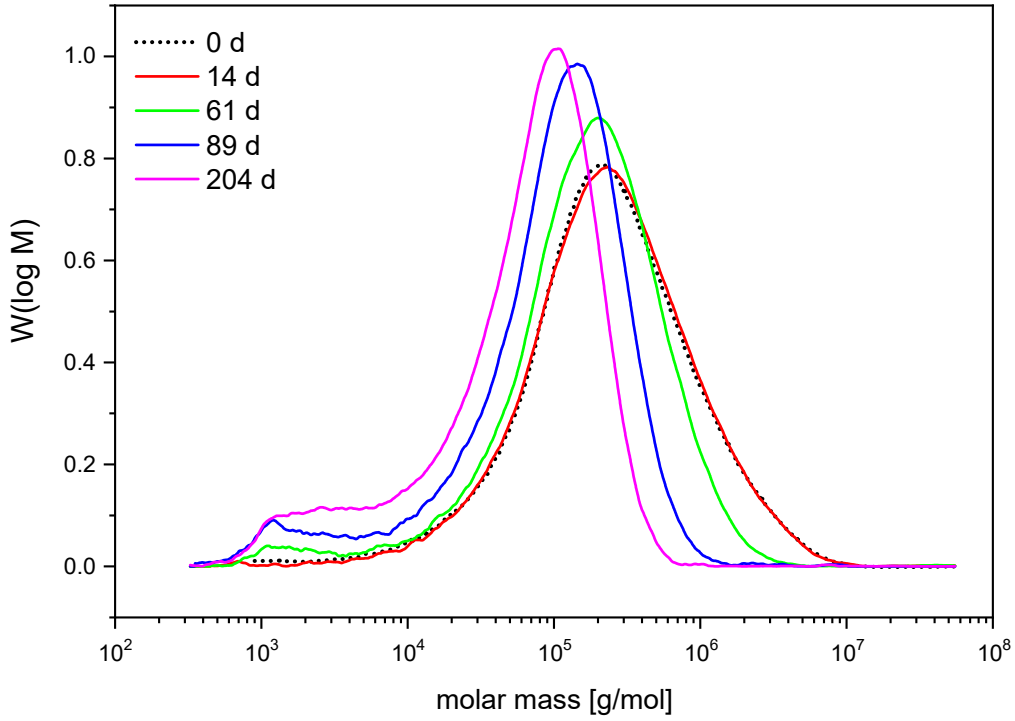

Figure 3. Decreasing molar mass of polypropylene geotextile over 204 days at 80 °C and 10 bar pressure.

The graph represents the resulting molar mass distributions of the geotextile after 14, 61, 89, and 204 days of aging. The baseline condition of the material is depicted by the dotted line representing the untreated geotextile before degradation in autoclaves. This shift indicates a decrease in the average molar mass, pointing to the fragmentation of longer polymer chains into shorter segments. In addition to relatively uniform chain scission, visible in the shift of the peak maximum, significant quantities of short-chain species are formed between 10^3 and 10^4 g/mol with an ongoing aging process. Such fragmentation signifies the aging process of the material, where the decrease in molar mass may lead to alterations in the geotextile's mechanical strength, elasticity, and permeability—attributes critical to its performance in engineering applications.

The SEC data thus reveal that while the chemical nature of the geotextile remains unchanged, the polymer chain length is reduced through the aging process induced in the autoclave. These modifications have the potential to impact the material's functional lifes-

pan. Accordingly, the observed degradation patterns are essential for evaluating geotextiles' long-term stability and applicability in enduring engineering structures. In SEC, which is a method for analyzing the molecular size distribution of polymers, three important parameters are often used to describe the molar mass distribution of the sample. These terms are statistical averages, and each gives different information about the polymer sample.

The number average molar mass M_n is the total weight of all the molecules in a sample divided by the total number of molecules. It is calculated by summing the products of the molar mass of each species and its mole fraction and then dividing by the sum of the mole fractions of all species. The weight average molar mass M_w is calculated by weighting the molar mass of each species by the fraction of the total weight that species represents. It gives more weight to heavier molecules and is generally higher than M_n for a polymer sample with a broad molar mass distribution. The z-average molar mass M_z is an even higher moment of the molar mass distribution and is significantly influenced by the presence of very high molar mass species in the sample.

In practical terms, M_n gives an idea of the average size of the molecules, M_w gives a sense of the distribution's breadth (especially the presence of high molar mass species), and M_z is particularly sensitive to the presence of very large molecules. These parameters are crucial in polymer science to understand the properties of polymer materials, as different molar mass distributions can lead to vastly different material properties. The following results are focused only on the weight average molar mass M_w and partially M_n; M_z was ignored.

Figure 4 illustrates the impact of temperature and pressure on degradation behavior, with a Boltzmann fit applied to demonstrate the molar mass trends across all conditions (data fit function in Origin 2020, OriginLab Corporation, for the sake of clarity in the figure only the results obtained with instrument BAM are displayed). The left side of the figure presents degradation kinetics under varying temperatures and pressures, clearly showing that temperature significantly influences the rate of degradation more than pressure. For instance, a higher temperature of 80 °C combined with a lower pressure of 30 bar results in greater degradation compared to a lower temperature of 70 °C and a higher pressure of 40 bar. The effect of different pressures alone is examined on the right side of the figure. It is observed that higher pressures, such as 30 bar, lead to more degradation than lower pressures of 20 or 10 bar, though the variation in degradation due to pressure changes is less pronounced than that caused by temperature changes.

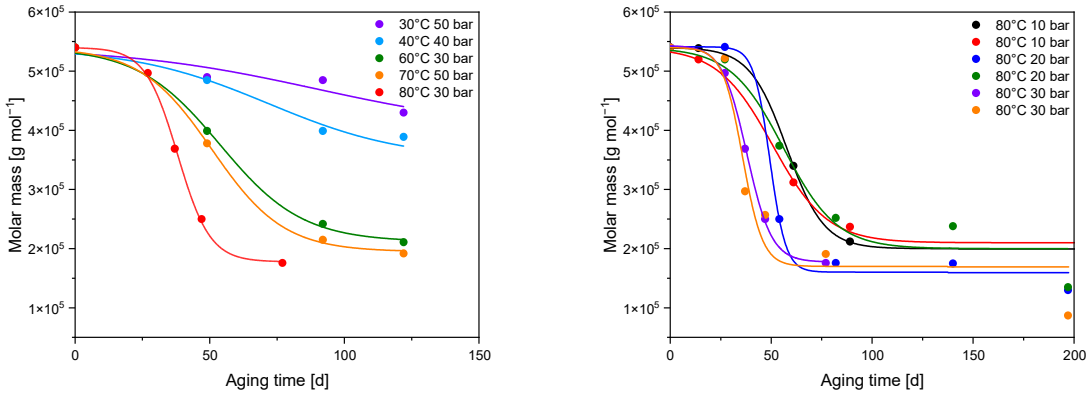

Figure 4. Molar mass Mw decrease over the time of 197 days at different temperatures between 40 and 80 °C and different pressures between 30 bar and 50 bar (**left**) and only at different pressures between 10 and 30 bar at 80 °C (**right**).

In this context, at all temperatures and pressures, a plateau was initially observed in the early stages of aging, where molar masses changed only slightly or not at all. This can be attributed to the use of phenolic and HAS. After approximately 30 days, there was an exponential decline in molar masses, with the degradation nearing completion around day 70. Following this period, similar to the initial stages, there was minimal to no further

reduction in molar masses. These trends were observed under all conditions tested, ranging between 10 and 50 bar and between 40 and 80 °C.

3.2. Accelerated Artificial Aging in Weathering Chambers at Increased Temperatures and UV Radiation

In addition to the aging process conducted in autoclaves, aging was also carried out in a weathering cabinet under UV exposure and in an oven at 80 °C under normal pressure. The profile of the average molar masses M_w and M_n over time is presented in Figure 5.

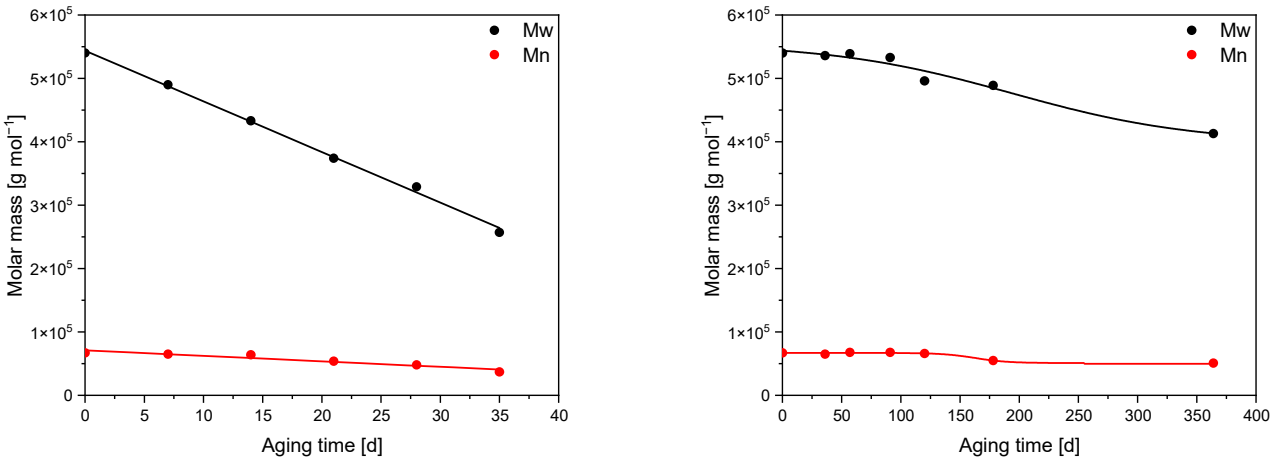

Figure 5. Molar mass Mw and Mn decrease over 35 days at UV-radiation (**left**) and over 364 days in an oven at 80 °C and normal pressure (**right**).

During UV aging, an almost linear decrease in molar masses was observed over 35 days, accompanied by slight yellowing of the geotextile material. In this relatively short period, M_w decreased from 540,000 to 257,000, effectively halving the molar mass. Similarly, M_n decreased from 67,000 to 37,000, representing a slightly smaller percentage decrease. In contrast to the aging in autoclaves, the initial stability and subsequent exponential decrease in molar masses were not observed in this case.

The aging process in the oven test at 80 °C in air under normal pressure over 364 days was comparatively mild. Here, the molar masses remained constant for 91 days, followed by a slight decrease from 540,000 to 413,000 for M_w and from 67,000 to 51,000 for M_n, amounting to a reduction of nearly 25%. Therefore, the molar mass degradation was significantly less pronounced during aging in the oven than under the increased pressures in autoclaves or UV exposure in the weathering cabinet.

For the UV-aged geotextiles and, for comparison, the PP pellets as well, the carbonyl index was determined using ATR-IR spectroscopy. The progression of the carbonyl index for both the aged geotextiles and the PP pellets is depicted in Figure 6.

In both materials, a logistic regression fit (fit function in Origin 2020) was employed to describe the trend of the carbonyl index. In the case of the geotextile, fit parameters of the PP pellets were used to obtain the geotextile fit because only three different exposure times for these measurements were available, which might have been insufficient to show the carbonyl index trend over time. The data revealed a comparatively strong increase within the first 7 days, reaching 0.18 for the geotextile and 0.25 for the PP pellets. Over the following 28 days, the rate of increase leveled off, resulting in a measured carbonyl index of 0.36, respectively 0.43 after 35 days of aging. This increase can be attributed to radical photo-oxidation of PP [32–34], during which carbonyl structures (ketones and aldehydes) are formed.

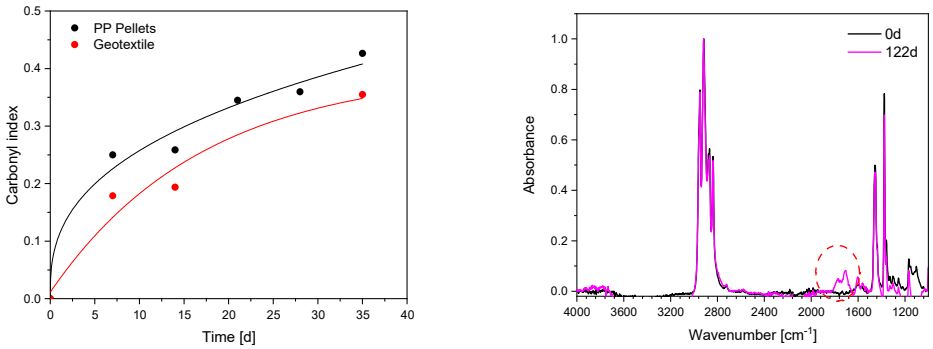

Figure 6. Carbonyl index increase over 35 days at UV-radiation, comparison between PP pellets and geotextile (**left**), ATR-IR spectrum aged (122 days) and unaged (black line, 0 d) geotextile. The carbonyl band of the aged sample is clearly visible at 1720 cm^{-1} (highlighted by red circle).

3.3. Determination of HAS-Stabilizer Behavior after Accelerated Artificial Aging

It was hypothesized that the initial constancy of molar mass observed during the aging of geotextiles in autoclaves and ovens could be attributed to the use or presence of stabilizers in the geotextiles. Typical HAS expected in this context include Chimassorb 944 and Chimassorb 2020, the structures of which are depicted in the subsequent Figure 7.

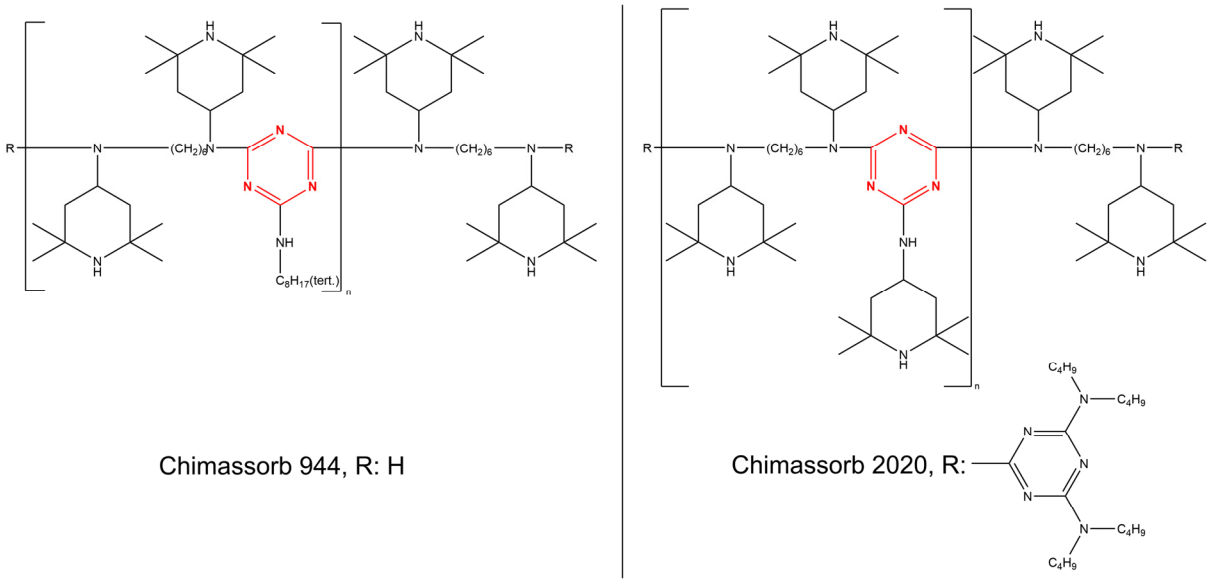

Figure 7. Structure of Chimassorb 944 (**left**) and Chimassorb 2020 (**right**), which are typically used as HAS in polymers. Triazine ring structure is highlighted (red).

From their structures, it can be inferred that both are polymers themselves. To identify these stabilizers, they were extracted from the geotextiles, analyzed qualitatively using ATR-IR-spectroscopy, and compared with the neat substances Chimassorb 944 and Chimassorb 2020, as shown in Figure 8.

In the extracted geotextile, two distinct absorption bands were noted at 1100 cm^{-1} and 1732 cm^{-1}, which were not present in both HAS pure substances. These bands can be attributed to impurities in the extraction or oxidation products in the geotextile. Aside from these, the spectrum of the geotextile closely resembles that of Chimassorb 944. In contrast, Chimassorb 2020 lacks the bands at 1567 cm^{-1} and 1219 cm^{-1}, and the bands at 1239 cm^{-1}, 1363 cm^{-1}, and 1471 cm^{-1} are less pronounced compared to Chimassorb 944 and the extracted geotextile. Therefore, it can be concluded that most probably Chimassorb 944 was used as HAS in the manufacturing of the geotextile. A verification with mass spectrometry was not performed within this study.

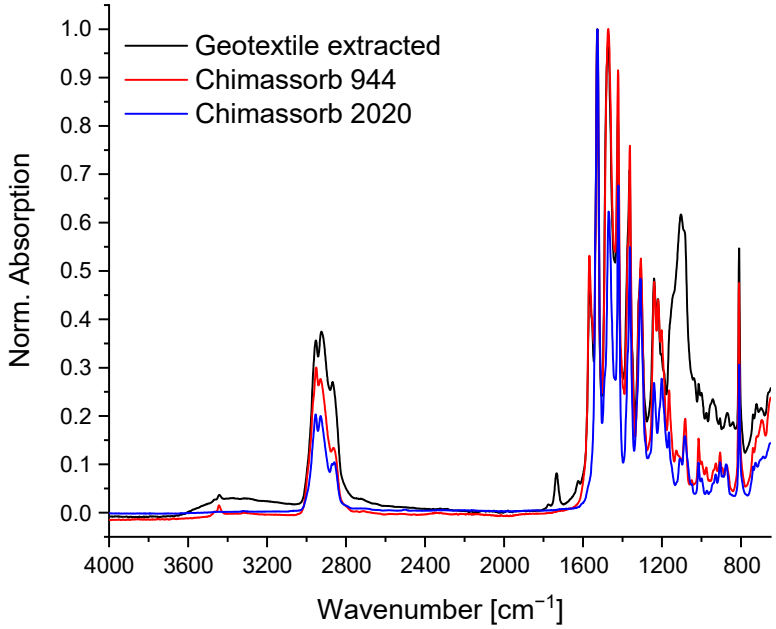

Figure 8. Comparison of extracted additives of the investigated geotextile and Chimassorb 944/Chimassorb 2020 pure substances.

After qualitatively identifying Chimassorb 944 as the HAS in geotextiles, quantification was subsequently carried out through extraction followed by UV/Vis spectroscopy (Freitag method) and HPLC. The yield of the extraction process is unknown, but the concentrations presented considered an extraction yield of 100%. It is important to note that the quantification with UV/Vis spectroscopy relies on the absorption band of the triazine ring in Chimassorb 944 (see Figure 7, highlighted part of the structure), although other HAS like Chimassorb 2020 also contain the triazine ring. Therefore, the total sum of all additives present in the geotextile was determined. The following Figure 9 presents the concentration profile of HAS in geotextiles, determined using UV/Vis spectroscopy and a diode array detector coupled with HPLC (for separation from other sample compounds, hereafter this method is abbreviated as HPLC) after aging in autoclaves at various temperatures and pressures, along with a comparison of the two quantification methods.

Starting from an initial concentration of 0.2% in the original geotextile, which was used for normalization, a lesser decrease in HAS concentration over a period of 124 days was observed at lower exposure temperatures, as expected. It is notable that sample (3) deviates from samples (1) and (2), particularly at 70 °C and 50 bar, despite all three samples being aged under the same conditions but in different autoclaves. This discrepancy may be attributed to variations in experimental conditions during the aging process. The last data point (in orange color) in the curve for 70 °C and 50 bar was regarded as an outlier. It was noted that the Freitag method, employing UV/Vis spectroscopy, generally yielded higher HAS concentrations compared to HPLC, where the peak area measured the concentration of Chimassorb 944 at a certain retention time in the chromatogram. At higher temperatures starting from 60 °C, there was a more significant decrease in HAS concentration, with UV/Vis spectroscopy showing a reduction to about 13% of the original value. In contrast, the concentration measured by HPLC typically dropped to zero within 49 or 92 days at temperatures above 60 °C, with no detectable signal for Chimassorb 944 in the chromatogram. The comparison between UV/Vis spectroscopy and HPLC revealed that almost all measured values were above the plotted line, indicating that UV/Vis spectroscopy detected higher HAS levels than the concentrations of Chimassorb 944 measured by HPLC. Further, it can be concluded that low HAS concentrations cannot be measured correctly using the Freitag method. The Freitag method still shows concentration results between 0.025 and 0.075% when the HPLC method could not detect any HAS. The

Freitag method was calibrated in a range of 0.011 to 0.2%, which means all measured Chimassorb concentrations were covered by the calibration curve. However, in the case of degraded HAS, where the triazine structure is still intact, the Freitag does not yield correct results. Therefore, the Freitag method might not be suitable for aged geotextile. Obviously, the method was developed for quality assurance in production only.

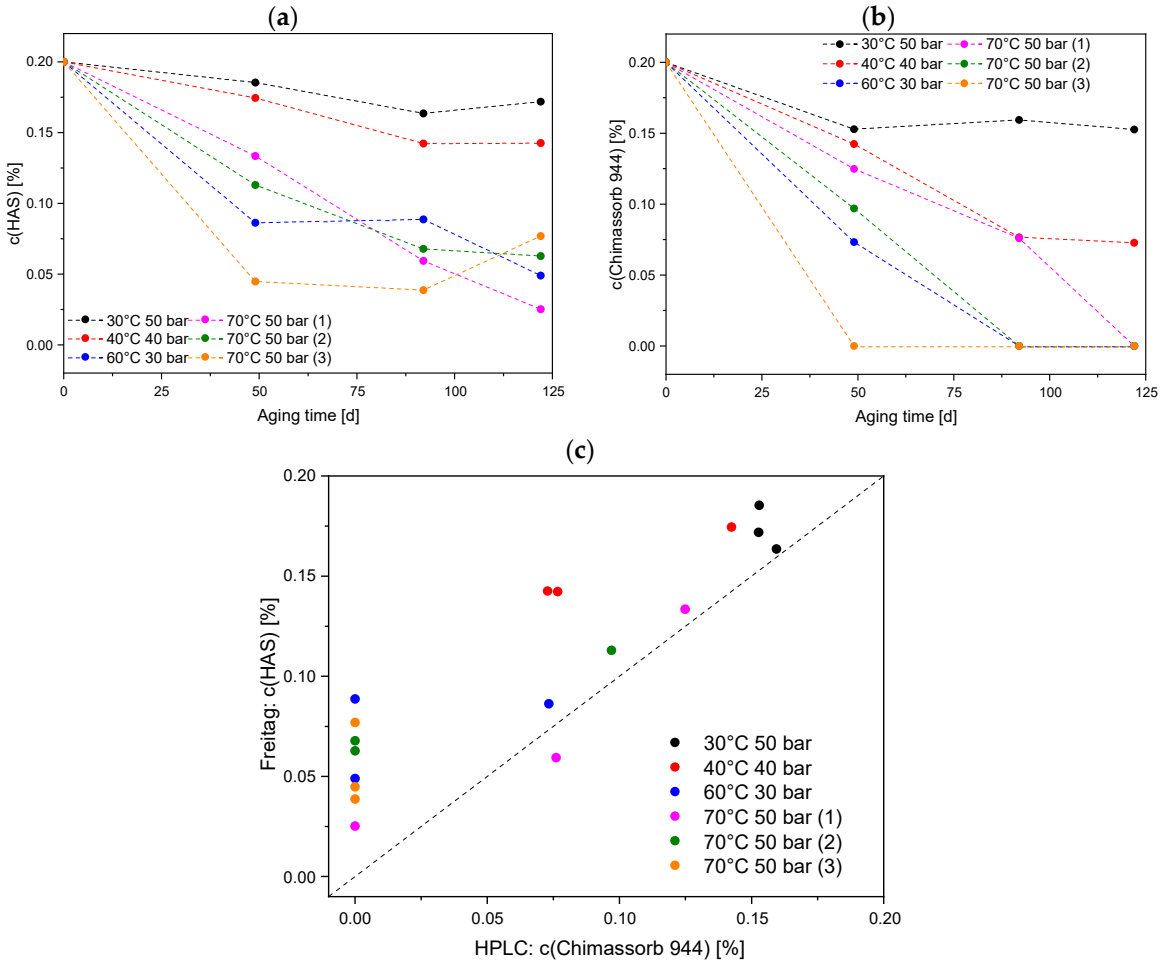

Figure 9. Decrease in concentration of HAS over time in geotextiles artificially aged in autoclaves at different conditions using extraction method and UV/Vis spectroscopy (Freitag method, (**a**)) and Chimassorb 944 concentration decrease over time in the same samples using HPLC (**b**). Comparison of determined HAS/Chimassorb 944 concentrations using the Freitag method vs. HPLC (**c**).

4. Discussion and Conclusions

Artificial aging in autoclaves under water at elevated temperatures and pressures has demonstrated that increased pressure alone does not significantly initiate the aging of geotextiles in terms of molar mass reduction. Elevated temperatures themselves also had a relatively minor impact on molar mass, as evidenced by aging in an oven at 80 °C, which showed little to no change in molar masses even after one year. In contrast, aging at comparable temperatures in autoclaves resulted in a more noticeable reduction in molar mass, likely influenced by the closed system and storage under water. Under all conditions described thus far, there was virtually no reduction in molar masses at the onset of aging, attributable to the use of stabilizers or additives in the geotextiles. The degradation of molar mass began only after the stabilizer was damaged or had diffused out of the material. On the other hand, aging under UV radiation showed a significant reduction in molar mass after just one week, with no initial phase of stability in molar masses.

The HAS Chimassorb 944 was identified as a stabilizer in the geotextile, which was practically undetectable using HPLC after the long-term aging in autoclaves at elevated

temperatures. Conversely, the triazine absorption band in Chimassorb 944 in the Freitag method remains detectable via UV/Vis spectroscopy. This suggests that during the aging of the geotextile, the HAS not only diffused out of the material but was likely damaged and decomposed while the triazine structure remained intact. Therefore, the Freitag method can be used for quality control in geotextile production but not for the estimation of the residual stabilizer content of exposed samples.

Degradation products of HAS in polymer samples subjected to accelerated weathering have been observed in mass spectrometry studies supporting this explanation [35]. Degradation of the PP can lead to fragmentation. It was estimated that PP degrades six times faster than polystyrene [10].

Carneiro et al. suggested using a combination of HAS and carbon black (a pigment that also provides protection against UV radiation) in geotextiles for use in marine environments. This could retain the material's properties when HAS is no longer functioning. However, an earlier publication showed that a black geomat made of PP lost up to 72% of its elasticity after use in a mostly uncovered application [36]. An also examined geotextile exhibited a much lower strain at the break while crystallinity was increased.

For the application of geotextiles, these results imply that uncovered applications where the material is exposed to the sun's UV radiation could be problematic and might require removal or replacement. Conversely, underground applications (e.g., geotextiles covered with sand) should be able to be used without issues over a long period, though even here, UV exposure during the mounting procedure must be avoided by not leaving the material uncovered outdoors at any time. Civil engineering constructions built with geotextiles have a low carbon footprint and are, therefore, more sustainable than alternatives with mineral material [37–40]. However, the observed construction at the Baltic shore near Swetlogorsk (see Figure 1) is not a best practice example for using geotextiles. Despite a lot of literature on the commercial use of geosynthetics in engineering, there is a lack of understanding of the environmental aspects associated with the use of geosynthetics and their end-of-life [41]. Testing methods for the durability and degradation of geosynthetics are of utmost importance, especially for the sustainability of the practical application. In all, the autoclave testing showed that it was able to achieve a suitable acceleration of the aging of the geotextiles investigated, while a weathering test might complement it in cases where UV exposure (during service life and before) cannot be excluded. The oven test did not accomplish the necessary acceleration of aging, even at the high temperature of 80 °C.

Author Contributions: Conceptualization, F.-G.S. and R.B.; methodology, P.S., J.F., V.W. and F.-G.S.; validation, P.S., J.F., V.W., R.B. and F.-G.S.; formal analysis, P.S. and F.-G.S.; investigation, F.-G.S.; writing—original draft preparation, P.S. and F.-G.S.; writing—review and editing, P.S., J.F., V.W., R.B. and F.-G.S.; visualization, P.S.; supervision, F.-G.S.; project administration, F.-G.S.; funding acquisition, F.-G.S. All authors have read and agreed to the published version of the manuscript.

Funding: This research was partly funded within the ERANET-RUS plus joint project EI-GEO, ID 212 (BMBF 01DJ18005).

Institutional Review Board Statement: Not applicable.

Informed Consent Statement: Not applicable.

Data Availability Statement: The raw data supporting the conclusions of this article will be made available by the authors upon request.

Acknowledgments: Part of the experimental work has been performed by Anna Böwe, Bianca Coesfeld and Anett Myxa.

Conflicts of Interest: The authors declare no conflicts of interest.

References

1. Wu, H.; Yao, C.; Li, C.; Miao, M.; Zhong, Y.; Lu, Y.; Liu, T. Review of Application and Innovation of Geotextiles in Geotechnical Engineering. *Materials* **2020**, *13*, 1774. [CrossRef] [PubMed]
2. Müller, W.W.; Saathoff, F. Geosynthetics in geoenvironmental engineering. *Sci. Technol. Adv. Mater.* **2015**, *16*, 034605. [CrossRef]

3. Ashis, M. Application of Geotextiles in Coastal Protection and Coastal Engineering Works: An overview. *Int. Res. J. Environ. Sci.* **2015**, *4*, 96–103.
4. Heibaum, M. The use of geosynthetics in scour protection. In *3rd International Conference on Scour and Erosion (ICSE-3)*; Verheij, H.J., Hoffmans, G.J., Eds.; CURNET: Gouda, The Netherlands, 2006.
5. Li, Y.; You, Z.-J.; Ma, Y.; Ren, B. Quantitative assessment of the shoreline protection performance of geotextile sandbags at an in-situ coastal experimental station. *Geotext. Geomembr.* **2023**, *51*, 371–380. [CrossRef]
6. Saathoff, F.; Oumeraci, H.; Restall, S. Australian and German experiences on the use of geotextile containers. *Geotext. Geomembr.* **2007**, *25*, 251–263. [CrossRef]
7. Hornsey, W.P.; Carley, J.T.; Coghlan, I.R.; Cox, R.J. Geotextile sand container shoreline protection systems: Design and application. *Geotext. Geomembr.* **2011**, *29*, 425–439. [CrossRef]
8. Koerner, R.M.; Hsuan, Y.G.; Koerner, G.R. Lifetime predictions of exposed geotextiles and geomembranes. *Geosynth. Int.* **2017**, *24*, 198–212. [CrossRef]
9. Carneiro, J.R.; Morais, M.; Lopes, M.d.L. Degradation of polypropylene geotextiles with different chemical stabilisations in marine environments. *Constr. Build. Mater.* **2018**, *165*, 877–886. [CrossRef]
10. Meides, N.; Mauel, A.; Menzel, T.; Altstädt, V.; Ruckdäschel, H.; Senker, J.; Strohriegl, P. Quantifying the fragmentation of polypropylene upon exposure to accelerated weathering. *Microplast. Nanoplast.* **2022**, *2*, 23. [CrossRef]
11. Schwarzenbach, K.; Gilg, B.; Müller, D.; Knobloch, G.; Pauquet, J.-R.; Rota-Graziosi, P.; Schmitter, A.; Zingg, J.; Kramer, E. Antioxidants. In *Plastics Additives Handbook*; Zweifel, H., Maier, R.D., Schiller, M., Eds.; Hanser: München, Germany, 2009; pp. 1–138.
12. Gensler, R.; Plummer, C.J.G.; Kausch, H.H.; Kramer, E.; Pauquet, J.R.; Zweifel, H. Thermo-oxidative degradation of isotactic polypropylene at high temperatures: Phenolic antioxidants versus HAS. *Polym. Degrad. Stab.* **2000**, *67*, 195–208. [CrossRef]
13. Gijsman, P. A review on the mechanism of action and applicability of Hindered Amine Stabilizers. *Polym. Degrad. Stab.* **2017**, *145*, 2–10. [CrossRef]
14. Heindl, M.; Zanzinger, H.; Zahn, A.; Schönlein, A. Study of artificial and outdoor weathering of stabilised polypropylene geotextiles. In Proceedings of the 4th European Geosynthetics Conference (EuroGeo 4), Edinbourgh, UK, 7–10 September 2008; Dixon, N., Ed.; International Geosynthetics Society: Austin, TX, USA, 2008.
15. Scholz, P.; Putna-Nimane, I.; Barda, I.; Liepina-Leimane, I.; Strode, E.; Kileso, A.; Esiukova, E.; Chubarenko, B.; Purina, I.; Simon, F.-G. Environmental Impact of Geosynthetics in Coastal Protection. *Materials* **2021**, *14*, 634. [CrossRef] [PubMed]
16. Gijsman, P.; Meijers, G.; Vitarelli, G. Comparison of the UV-degradation chemistry of polypropylene, polyethylene, polyamide 6 and polybutylene terephthalate. *Polym. Degrad. Stab.* **1999**, *65*, 433–441. [CrossRef]
17. Striegel, A.M.; Yau, W.W.; Kirkland, J.J.; Bly, D.D. *Modern Size-Exclusion Liquid Chromatography, Practice of Gel Permeation and Gel Filtration Chromatography*, 2nd ed.; John Wiley & Sons: Hoboken, NJ, USA, 2009.
18. Almond, J.; Sugumaar, P.; Wenzel, M.N.; Hill, G.; Wallis, C. Determination of the carbonyl index of polyethylene and polypropylene using specified area under band methodology with ATR-FTIR spectroscopy. *e-Polymers* **2020**, *20*, 369–381. [CrossRef]
19. Robertson, D. The Oxidative Resistance of Polymeric Geosynthetic Barriers (Gbr-P) Used for Road and Railway Tunnels. *Polym. Test.* **2013**, *32*, 1594–1602. [CrossRef]
20. *DIN EN ISO 13438*; Geotextiles and Geotextile-Related Products—Screening Test Method for Determining the Resistance to Oxidation. Beuth-Verlag: Berlin, Germany, 2005.
21. Richaud, E.; Farcas, F.; Divet, L.; Paul Benneton, J. Accelerated ageing of polypropylene geotextiles, the effect of temperature, oxygen pressure and aqueous media on fibers—Methodological aspects. *Geotext. Geomembr.* **2008**, *26*, 71–81. [CrossRef]
22. Müller, W.W.; Jakob, I.; Tatzky-Gerth, R.; Wöhlecke, A. A Study on Antioxidant Depletion and Degradation in Polyolefin-Based Geosynthetics: Sacrificial Versus Regenerative Stabilization. *Polym. Eng. Sci.* **2016**, *56*, 129–142. [CrossRef]
23. Bandow, N.; Will, V.; Wachtendorf, V.; Simon, F.G. Contaminant release from aged microplastic. *Environ. Chem.* **2017**, *14*, 394–405. [CrossRef]
24. Wypych, G. *Handbook of Material Weathering*, 5th ed.; Elsevier: Oxford, UK, 2013; ISBN 978-1-895198-62-1. [CrossRef]
25. *DIN EN ISO 4892-3*; Plastics—Methods of Exposure to Laboratory Light Sources—Part 3: Fluorescent UV Lamps. Beuth-Verlag: Berlin, Germany, 2016.
26. Geburtig, A.; Wachtendorf, V.; Falkenhagen, J. Combined impact of UV radiation and nitric acid on high-density polyethylene containers as a laboratory test. *Packag. Technol. Sci.* **2022**, *35*, 729–735. [CrossRef]
27. Monrabal, B.; Sancho-Tello, J. High Temperature GPC Analysis of Polyolefins with Infrared Detection. *LC GC Asia Pac.* **2009**, *12*, 58–59.
28. Freitag, W. Determination of a polymeric light stabiliser (Chimassorb 944) in polypropylene. *Fresenius' Z. Für Anal. Chem.* **1983**, *316*, 495–496. [CrossRef]
29. Ali Farajzadeh, M.; Eskandar, S.G.; Ranji, A.; Feyz, E. HPLC technique for quantitation of Chimassorb 944, and its evaluation in analysis of real and standard samples of polyolefins. *Microchim. Acta* **2007**, *159*, 363–369. [CrossRef]
30. Valente, I.M.; Carneiro, J.R.; Almeida, P.J.; Lopes, M.d.L. Determination of Chimassorb 944 in polypropylene geotextiles by HPLC-UV. *Anal. Lett.* **2011**, *44*, 617–625. [CrossRef]

31. Coulier, L.; Kaal, E.R.; Tienstra, M.; Hankemeier, T. Identification and quantification of (polymeric) hindered-amine light stabilizers in polymers using pyrolysis-gas chromatography-mass spectrometry and liquid chromatography-ultraviolet absorbance detection-evaporative light scattering detection. *J. Chromatogr. A* **2005**, *1062*, 227–238. [CrossRef] [PubMed]
32. Kato, Y.; Carlsson, D.J.; Wiles, D.M. The photo-oxidation of polypropylene: Some effects of molecular order. *J. Appl. Polym. Sci.* **1969**, *13*, 1447–1458. [CrossRef]
33. Yakimets, I.; Lai, D.; Guigon, M. Effect of photo-oxidation cracks on behaviour of thick polypropylene samples. *Polym. Degrad. Stab.* **2004**, *86*, 59–67. [CrossRef]
34. Carlsson, D.J.; Wiles, D.M. The Photooxidative Degradation of Polypropylene. Part I. Photooxidation and Photoinitiation Processes. *J. Macromol. Sci. Part C* **1976**, *14*, 65–106. [CrossRef]
35. Paine, M.R.L.; Barker, P.J.; Maclauglin, S.A.; Mitchell, T.W.; Blanksby, S.J. Direct detection of additives and degradation products from polymers by liquid extraction surface analysis employing chip-based nanospray mass spectrometry. *Rapid Commun. Mass Spectrom.* **2012**, *26*, 412–418. [CrossRef] [PubMed]
36. Chubarenko, B.; Domnin, D.; Simon, F.-G.; Scholz, P.; Leitsin, V.; Tovpinets, A.; Karmanov, K.; Esiukova, E. Change over Time in the Mechanical Properties of Geosynthetics Used in Coastal Protection in the South-Eastern Baltic. *J. Mar. Sci. Eng.* **2023**, *11*, 113. [CrossRef]
37. Heerten, G. Reduction of climate-damaging gases in geotechnical engineering practice using geosynthetics. *Geotext. Geomembr.* **2012**, *30*, 43–49. [CrossRef]
38. Frischknecht, R.; Stucki, M.; Büsser, S.; Itten, R.; Wallbaum, H. Comparative life cycle assessment of geosynthetics versus conventional construction materials. *Ground Eng.* **2011**, *45*, 24–28.
39. Dixon, N.; Raja, J.; Fowmes, G.; Frost, M. 26—Sustainability aspects of using geotextiles. In *Geotextiles*; Koerner, R.M., Ed.; Woodhead Publishing: Sawston, UK, 2016; pp. 577–596. [CrossRef]
40. Dąbrowska, J.; Kiersnowska, A.; Zięba, Z.; Trach, Y. Sustainability of Geosynthetics-Based Solutions. *Environments* **2023**, *10*, 64. [CrossRef]
41. Giglio, C.; Vocaturo, G.S.; Palmieri, R. A Scientometric Study of LCA-Based Industrialization and Commercialization of Geosynthetics in Infrastructures. *Appl. Sci.* **2023**, *13*, 2328. [CrossRef]